

# An EEG Coherence Based Method Used for Mental Tasks Classification

Dan-Marius Dobrea\*, Monica-Claudia Dobrea\*, Mihaela Costin\*\*

\*Faculty of Electronics and Telecommunications, "Gh. Asachi" Technical University, Iasi, Romania

\*\* Computer Science Institute, Romanian Academy (IIT) Iasi

**Abstract**-In this paper a new coherence based method to extract the appropriate EEG features for a five mental tasks classification problem is proposed. The new introduced method has the advantage of using an adaptive new technique that models the EEG signal using the frequency information obtained by employing the coherence function to each EEG recording channel. The adaptive attribute of the technique is due to both, to the amplitude and, respective, to the phase adaptive processes used to model the EEG signal. Another specificity of the new modeling technique is given by the fact of exploiting the nonlinear dynamics of the brain system; this is reflected in the particular spectral mixing of the fundamental spectral components obtained first, by using the coherence function. Finally, to conclude the obtained results in comparison with the results reported in the literature, by using this new approach the classification rate was noticeably improved.

## I. INTRODUCTION

An important and challenging biomedical signal processing problem in the brain-computer interface (BCI) field of research is the mental task classification by recognizing the electroencephalographic (EEG) patterns. The most frequently used means for this are: the slow cortical potentials [1], [2], the P300 evoked potentials [1], [2], [3], [4], the EEG signal acquired at the sensori-motor cortex level [1], [5], [6], the visual evoked potentials [2] and by means of cortical neurons [2]. All these represent particular useful information that was further used, in different researches, as input data for the classifying process.

Now, it is largely recognized that the decisions made as the BCI output are mainly affected by the accuracy of classification. On the other hand, this last one essentially depends on the quality of the EEG signal (including here the appropriate number and locations of the EEG channels [7]) and the used processing algorithms (corresponding to the preprocessing, feature extraction [8], [9] and feature classification stages [10], [11]). Knowing the aphorism "garbage in, garbage out", a main attention was given to find, first, which is the best useful information for the particular classification challenge and, second, to find those methods that are suitable for extracting this information from the raw EEG signals. Until now a number of specific features and methods were proposed. The most frequently used features in the BCI systems are: AR coefficients [12], [13], AR models with exogenous inputs [13], power spectral parameters [14], statistic phase synchronization [14], [15], spatial filtering, mean value of the phase coherence [14], discharge frequency

of a neuronal group [16], P300 wave [1], [17] etc.

Besides these researches there are also papers that focused only on finding those approaches that allow for an online training of the classifiers [18] while others concentrated on choosing the appropriate classifier [19] or the optimal mental tasks for classification in BCIs. Anyway, the shared goal of all of the papers mentioned above is the improvement of BCI systems.

In the study presented below we introduce a new method for EEG feature extraction. The analysis was done using the Purdue dataset that is one of the two known and well established datasets in the BCI field, the other being the Graz dataset. Both datasets are accessible from internet [20].

The EEG signals, recorded from six different cortical locations and corresponding to four subjects and to five different tasks, were modeled by using a derived version of the Adaptive Nonlinear Markov Process Amplitude (ANMPA) method presented in [16]. This model will be named in the rest of the paper Adaptive Amplitude and Phase Process Model (AAPP). Also, the spontaneous oscillations (a priori specified) used in this model were determined by making use of the coherence function applied to each individual recording channel, for each mental task and for each subject. The parameters of the AAPP model were then used as input data to a multilayer perceptron whose output finally provided the correct classification rate for all tasks and for each particular subject. In this way we addressed to those BCI systems dedicated to a single person and to a limited number of different mental tasks. Usually, the BCI applications focus on one subject and one or more pairs of mental tasks [21], [22], and rarely on three [23], four or even five tasks [24] simultaneously. In our study we will present the results obtained for only one of the four subjects (namely, the subject that better performed the mental tasks) and for all the five cognitive tasks.

## II. MATERIALS AND METHODS

### A. Data Acquisition

EEG data were recorded from 6 electrodes placed at locations according to the International 10-20 system, Fig. 1, each pair of them being fixed on the scalp, on the central (C3, C4), the parietal (P3, P4) and the occipital (O1, O2) positions as shown in Fig. 1. All channels were referred to the right mastoid A2 and were digitally sampled at 250 Hz. The total time of each recording was 10 s.

Data from four subjects, performing five mental tasks that

involved different cognitive abilities, were analyzed. The tasks, done without vocalizing and with the eyes closed, are as follows: the baseline task (the subject relaxed as much as possible); the letter task (the subject mentally composed a letter to a friend); the counting task (the subject watched sequentially numbers written on an imaginary blackboard); the math task (the subject performed a nontrivial multiplication) and the rotation task (the subject studied for 30 seconds a three dimensional object and, with the object being removed, was asked to imaginary rotate it about an axis).

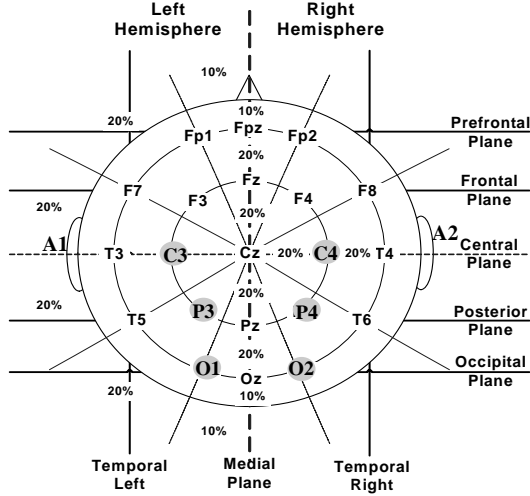


Fig. 1. The electrodes positions

### B. Coherence Function

As we have already mentioned above, we used the coherence function in order to determine the spontaneous oscillations that are a priori specified to the AAPP model. In order to obtain the formula for the coherence function we first divided each of the two analyzed time series (of length  $P$ ) into overlapping sections; thus we obtained  $L$  sections, each of length  $T$  for each time series. Time series data from each section were Fourier-transformed, giving a frequency resolution  $df$ . No tapering or weighting function was used. The finite Fourier transform of the  $l$ th segment ( $l=1 \dots L$ ) from each time series at frequency  $\lambda$  was denoted by  $F_x^T(\lambda, l)$  and defined as:

$$F_x^T(\lambda, l) = \int_{(l-1)T}^{lT} x(t) e^{-i\lambda t} dt \approx \sum_{t=(l-1)T}^{lT} e^{-i\lambda t} x(t) \quad (1)$$

where:  $x(t)$  is replaced in our case by  $s_1(t)$  – the first trial for

each subject, each task and each EEG channel and respectively, by  $s_2(t)$  – the second trial for the same subject, task and channel.

Auto- and cross-spectra were, then, estimated by averaging over the overlapped sections:

$$\hat{f}_{xy}(\lambda) = \frac{1}{2\pi LT} \sum_{l=1}^L F_x^T(\lambda, l) \overline{F_y^T(\lambda, l)} \quad (2)$$

where: the overbar  $\overline{\phantom{x}}$  on  $F_y^T(\lambda, l)$  indicates a complex conjugate and  $(x, y)$  are the pairs  $(s_1, s_2)$  for cross-spectra, and  $(s_1, s_2)$ , respectively  $(s_1, s_2)$  for autospectra. Further, the coherence estimate for two signals was computed using the formula:

$$\left| \hat{R}_{xy}(\lambda) \right|^2 = \frac{\left| \hat{f}_{xy}(\lambda) \right|^2}{\hat{f}_{xx}(\lambda) \hat{f}_{yy}(\lambda)} \quad (3)$$

The coherence function indicates the degree of linear correlation in the frequency domain between two signals on a scale from zero (independence) to one (complete linear dependence). By taking the square root of (3) we obtained the complex valued function named coherency. Further we applied Fisher's transform ( $\text{Tanh}^{-1}$ ) to the magnitude of the estimated coherency and obtained a new variable whose variance is given by the constant value:  $\sigma^2 = 1/2L$ ; here,  $L$  is the number of the sections used to estimate the coherence. Based on these we calculated a statistical test to assess that the individual coherence estimates for all the pairs  $(s_1, s_2)$  have a common mean. For the  $k$  coherency estimates,  $m_i$ , we estimated the common mean as:

$$\bar{m} = \sum_{i=1}^k \frac{m_i}{k} \quad (4)$$

and designed the statistics,

$$\sum_{i=1}^k \frac{(m_i - \bar{m})^2}{\sigma^2} \quad (5)$$

which under the null hypothesis is distributed approximately as  $\chi^2$  with  $(k-1)$  degrees of freedom. The computation of (5) was done separately at each frequency,  $\lambda$ , over the range  $[0, 125]$  Hz. A confidence limit at the 95% level was set at the value  $\chi^2(\alpha; k-1)$  and the null hypothesis was rejected if the (5) exceeded this limit.

In order to facilitate the interpretation we calculated with (6) the pooled coherence estimate, a parameter whose values

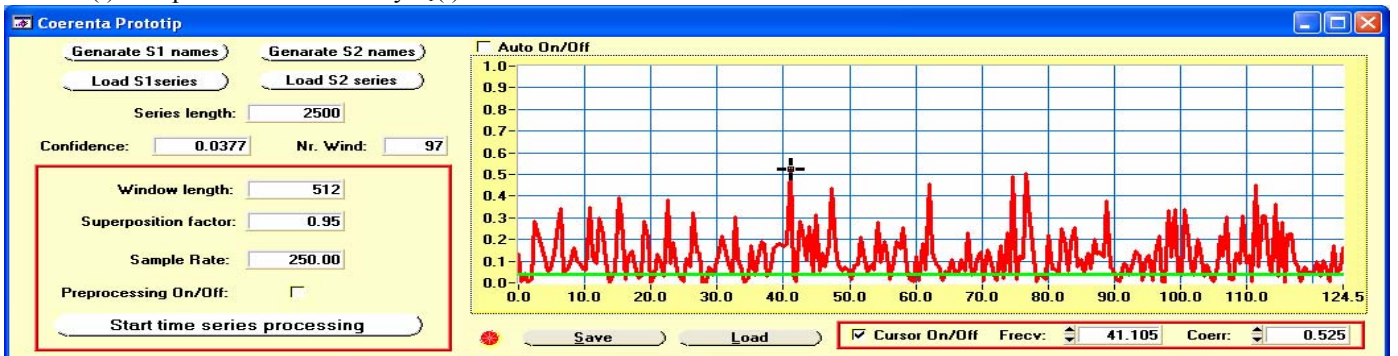


Fig. 2. The software user interface program used in coherence computation – the horizontal line is the confidence limit at the 95% level

range from 0 up to 1. Assuming the independence between the  $k$  pairs of processes, the upper 95% confidence limit for the estimate of (6) is given by (7).

$$\frac{\left| \sum_{i=1}^k \hat{f}_{xy(\lambda)} L \right|^2}{\left( \sum_{i=1}^k \hat{f}_{xx(\lambda)} L \right) \left( \sum_{i=1}^k \hat{f}_{yy(\lambda)} L \right)} \quad (6)$$

$$1 - (0.05) \frac{1}{\sum_{i=1}^k L - 1} \quad (7)$$

Values of the pooled estimate of coherence lying below this line can be taken as evidence that, on average, no coupling occurs between the two processes ( $x, y$ ) at a particular frequency  $\lambda$ . We can also interpret (6) as representative of each coherence estimate between the  $k$  processes only if the null hypothesis (the  $k$  transformed coherency estimates have a common mean) is accepted.

### C. Adaptive Amplitude and Phase Process Model

After determining the spontaneous EEG frequencies, an adaptive amplitude and phase model was implemented in order to model the original EEG data sets.

In a first implementation, the EEG signal was modeled using adaptive nonlinear Markov process amplitude (ANMPA). This model is an implementation of the nonlinear Markov process amplitude model (NMPA) proposed in [25] for nonlinear coupling interaction of spontaneous EEG. The model parameters were determined adaptively with the least mean square (LMS) algorithm. A version of this algorithm for a first-order Markov process amplitude model is presented in [26].

$$\left\{ \begin{array}{l} y[n] = \sum_{j=1}^K a_j[n] x_j[n] + \sum_{j=1}^K \varepsilon_j^s a_j[n] \alpha_j[n] + \\ \quad \sum_{\substack{i,j=1,K \\ i \neq j}} [\varepsilon_{ij}^{c1} a_i[n] a_j[n] \beta_{ij}[n] + \varepsilon_{ij}^{c2} a_i[n] a_j[n] \theta_{ij}[n]] \\ x_j[n] = \sin(n \cdot T_S \cdot 2\pi \cdot f_j + \phi_j) \\ \alpha_i[n] = \sin(n \cdot T_S \cdot 2\pi \cdot \underbrace{2f_j}_{f_i} + \phi_{ij}) \\ \beta_{ij}[n] = \sin[n \cdot T_S \cdot 2\pi \cdot (f_i - f_j) + \phi_{ij}] \\ \theta_{ij}[n] = \sin[n \cdot T_S \cdot 2\pi \cdot (f_i + f_j) + \phi_{ij}] \end{array} \right. \quad (8)$$

For our classification task, the EEG model was assumed to suitably decompose the frequency components of the EEG signal into some spontaneous oscillations (a priori specified) and the nonlinearly coupled frequencies (self-coupling oscillations and, respectively, cross-coupling oscillations). More exactly, two oscillatory waves (of  $f_1$  and  $f_2$  frequency) passing through a nonlinear square system generates two kinds

of harmonic frequencies: self-coupling harmonics ( $2 \cdot f_1$  and  $2 \cdot f_2$ ) and, respectively, cross-coupling harmonics ( $f_1 \pm f_2$ ).

Having this information we wrote the NMPA model as in (8). Here,  $y[n]$  is the estimated EEG signal assumed to be composed of  $K$  different oscillations ( $x_j, j=1 \div K$ ),  $T_S$  is the sampling rate,  $f_j$  is the dominant  $j$ th frequency,  $\phi_j$  is the initial phase (which was set to zero, being unused),  $\varepsilon_j^s$  is the self-coupling coefficient of the  $j$ th model oscillation,  $\varepsilon_{ij}^{c1}$  and  $\varepsilon_{ij}^{c2}$  are the cross-coupling coefficients of the coupled frequency  $-f_i - f_j$  and  $f_i + f_j$ , respectively,  $n$  is the time index and  $a_j[n]$  is the model amplitude of the first order Markov process.

The next estimate of the model amplitude  $a_j[n+1]$  was given by (9):

$$\begin{cases} a_j[n+1] = \gamma_j[n] \cdot a_j[n] + \mu_j[n] \cdot \xi_j[n] \\ 0 < \gamma_j[n] < 1 \end{cases} \quad (9)$$

where:  $\xi_j[n]$  is the independent increment of Gaussian distribution with zero mean and unity variance,  $\mu_j$  is the coefficient of the random process and  $\gamma_j$  is the coefficient of the first-order Markov process.

The least mean square (LMS) algorithm was used in order to adaptively estimate the model parameters ( $a_j, \gamma_j, \mu_j, \varepsilon_j^s, \varepsilon_{ij}^{c1}, \varepsilon_{ij}^{c2}$ ,  $i, j=1 \div K, i \neq j$ ). The error squared,  $e[n]^2 = [s[n] - y[n]]^2$  (where  $s[n]$  was the modeled EEG signal), was used as an estimate of the mean square error cost function  $J$ , defined as  $J = 1/2 \cdot E\{e[n]^2\}$ .

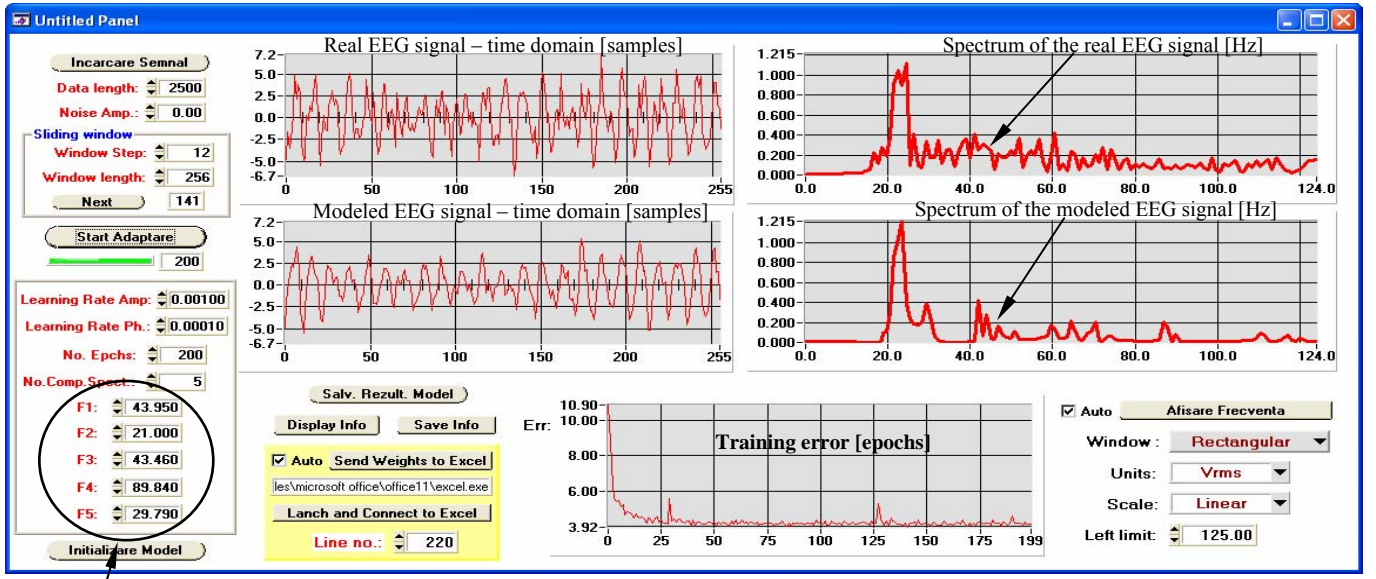
After a large number of tests and analyses we concluded that the ANMPA model had several major disadvantages. The most important of them was generated by its poor convergence characteristics. In order to obtain the best solution, a large number of ANMPA runnings had to be carried on. This fact was considered a big disadvantage of the ANMPA model, its using for a BCI system making the real time operating characteristics of this last one to be unpredictable.

$$\begin{aligned} y[n] &= \sum_{m=1}^K a_m[n] x_m[n] + \sum_{m=1}^L b_m[n] \alpha_m[n] + \\ &+ \sum_{\substack{l=1 \\ l \neq m}}^M \sum_{m=1}^N c_{lm}[n] \beta_{lm}[n] + \sum_{\substack{l=1 \\ l \neq m}}^P \sum_{m=1}^Q d_{lm}[n] \theta_{lm}[n] \end{aligned} \quad (10)$$

From these reasons and in order to improve the behavior of the ANMPA model, the estimated EEG signal,  $y[n]$ , was more directly computed, by using (10); also, the phases of each used oscillation, self-coupling harmonics and cross-coupling harmonics were adaptively find out.

The spectral components  $a_j[n]$ ,  $\alpha_i[n]$ ,  $\beta_{ij}[n]$  and  $\theta_{ij}[n]$  have the same form with the one presented in (8).

$$\begin{aligned} a_j[n] &= a_j[n] - \eta_{a_j} \frac{\partial \left\{ \frac{1}{2} e^2[n] \right\}}{\partial a_j[n]} = \\ &= a_j[n] + \eta_{a_j} e[n] \frac{\partial y[n]}{\partial a_j[n]} = \\ &= a_j[n] + \eta_{a_j} e[n] x_j[n] \end{aligned} \quad (11)$$



EEG spontaneous frequency values [Hz]

Fig. 3. The user interface for the AAPP software

On the other hand, the unknown amplitudes and phases were found by minimizing the power of the error  $e[n]$  – the cost function,  $J$ , as it was presented above.

Applying the LMS equations (11) and using (8), (10) we obtained the following adjusting formulas for the AAPP amplitude model parameters (see relations (12) or (13), (14), (15) and (16)):

$$a_j[n+1] = a_j[n] + \eta_{a_j} e[n] x_j[n] \quad (12)$$

or

$$a_j[n+1] = a_j[n] + \eta_{a_j} e[n] \sin(nT_s 2\pi \cdot f_j + \phi_j[n]) \quad (13)$$

$$b_j[n+1] = b_j[n] + \eta_{b_j} e[n] \alpha_j[n] \quad (14)$$

$$c_{ij}[n+1] = c_{ij}[n] + \eta_{c_{ij}} e[n] \beta_{ij}[n] \quad (15)$$

$$d_{ij}[n+1] = d_{ij}[n] + \eta_{d_{ij}} e[n] \theta_{ij}[n] \quad (16)$$

The quantity  $\eta_{a_j}$ ,  $\eta_{b_j}$ ,  $\eta_{c_{ij}}$  and  $\eta_{d_{ij}}$  are positive scalars that control the convergence rate and ensure the stability of the model. Regarding the phase variables, the applied Window's LMS relations were similar with the ones presented above, being given by (17):

$$\begin{aligned} \phi_j[n+1] &= \phi_j[n] - \eta_{\phi_j} \left\{ \frac{\partial \left( \frac{1}{2} e^2[n] \right)}{\partial \phi_j[n]} \right\} = \\ &= \phi_j[n] + \eta_{\phi_j} e[n] \frac{\partial y[n]}{\partial \phi_j[n]} \end{aligned} \quad (17)$$

$$\begin{aligned} \frac{\partial y[n]}{\partial \phi_j[n]} &= \frac{\partial (a_j[n] \sin(n \cdot T_s \cdot 2\pi \cdot f_j + \phi_j[n]))}{\partial \phi_j[n]} = \\ &= a_j[n] \cos(n \cdot T_s \cdot 2\pi \cdot f_j + \phi_j[n]) \end{aligned} \quad (18)$$

and finally:

$$\phi_j[n+1] = \phi_j[n] + \eta_{\phi_j} e[n] a_j[n] \cos(n \cdot T_s \cdot 2\pi \cdot f_j + \phi_j) \quad (19)$$

Based on the relations presented above one can notice that when the number of interfering sinusoids is small the computational complexity of the model is very low. In order to

update an estimated parameter, no more than 4 multiplications and 3 additions are needed for each sampling interval. The higher demand on computational complexity is given by the computation of sinus and cosines functions. But this problem can be easily solved using a look-up table.

To end with the new proposed EEG model, the most important advantage of the AAPP is given by its superior convergence characteristics. Actually, the model is able to converge to the optimal solution in no more than 30 sampling intervals (see Fig. 3). Both software applications, presented in Fig. 2 and Fig. 3, were developed in LabWindows CVI environment.

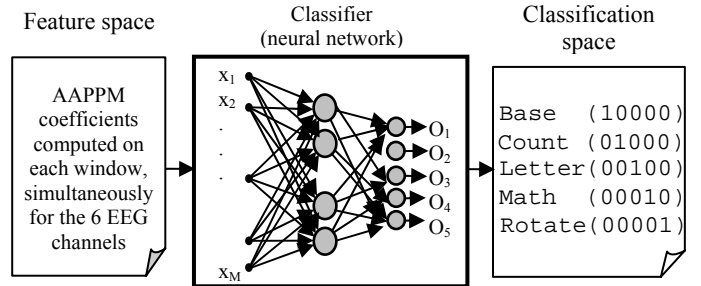


Fig. 4. The classification process

#### D. Artificial Neural Networks (ANNs)

The calculated AAPP coefficients represent the components of the ANN input feature-vectors. The nucleus of classification is based on a simple feedforward neural network of multilayer perceptron type (MLP), with only one hidden layer and trained with backpropagation algorithm [29]. The classifier uses the feature-vectors as shown in Fig. 4.

In this paper we preferred to use the MLP ANN instead of any other superior classifiers (like support vector machines etc.) only because we wished to test the new introduced concept and its performances in comparison with the other implemented feature extraction techniques and not the power of the classification systems.

In this paper all the neuronal structures were implemented and tested in NeuroSolutions environment.

### III. RESULTS

In the present study we focused only on one single subject, namely, subject 2 which was reported in the literature as having the greatest performances in comparison with the other 3 subjects.

To obtain the values of the coherence function, calculated for two different records acquired from the same scalp electrode, in the same recording conditions and for the same task, we used the sliding window method. The length of the windows was 512 samples overlapped by 95% (this means a sliding window of roughly 25 samples or, equivalent, 100 ms). In this way we intimately followed the course of the cortical activity transitions, considered to happen within time intervals of hundred of milliseconds.

The selection of the fundamental frequencies used a priori in the EEG AAPP model was done as follows. For each recording channel (C1, C2, P1, P2, O1, O2) five different frequencies were taken into account, each of them representing the frequency with the greatest coherence value obtained for the respective channel and for each of the five mental tasks. Here, we have to stress that all the selected frequencies were from the gamma band. This comes to emphasize the importance of the high frequencies band that until recently was considered not carrying any useful information. Nowadays there are researches that sustain this new innovative idea [21], [27].

The final feature vectors employed at the input of the ANN classifier were achieved by concatenating the parameters of the AAPP model obtained for EEG sliding windows of 256 samples length recorded simultaneously from the all six EEG channels. For a sliding window of 12 samples and for a length of 2250 samples for the 20 Hz high pass FIR filtered EEG signals, we finally got 1670 ANN input feature vectors (167 vectors/each recording \* 2 recordings \* 5 mental tasks). From this input database we used 80% data for the training set (1336 vectors) and 20% data for cross validation (CV) set (334 vectors). The necessity of pre-filtering the signals was given by the fact that the most part of the EEG signal energy (frequency peaks) is usually situated in the 0 – 20 Hz band, thus making us difficult to obtain a reliable AAPP model for the EEG signal. Additionally, in order that the proposed AAPP model to not introduce frequencies within 0 – 20 Hz band or over the half of the sampling frequency (namely, 125 Hz), we revised the initial soft for the model and forced all the learning rates and the initial amplitude values to became zero but only for those derived frequencies within the already mentioned values intervals. Thus, by removing the frequency components of zero value the feature vectors were reduced from the 180 components to only 104 components.

Regarding the architecture of the MLP network, we chose an one hidden layer ANN, with 104 inputs, 40 processing elements on the hidden layer and 4 and 5 outputs corresponding to the cases with 4 and, respectively 5 mental tasks classification. The desired data set were constructed as it was shown in Fig. 4. MLP networks with 2 hidden layers were

also analyzed but there was no any improvement in the obtained performances.

The results achieved for the two analyzed cases (4 tasks and, respectively, 5 tasks classification problem) are given in Tabel 1 and, correspondingly in Table 2. In both tables the tasks are represented as follows: T1 – baseline, T2 – count, T3 – letter, T4 – math and T5 – rotate.

TABLE I  
THE CONFUSION MATRIX FOR THE 4 TASKS CLASSIFICATION CASE

		Assigned classes			
		T2	T3	T4	T5
Real classes	T2	79.6%	3.2%	6.3%	10.9%
	T3	2.9%	84.1%	5.7%	7.3%
	T4	6.1%	13.6%	77.3%	3%
	T5	14.7%	10.3%	2.9%	72.1%

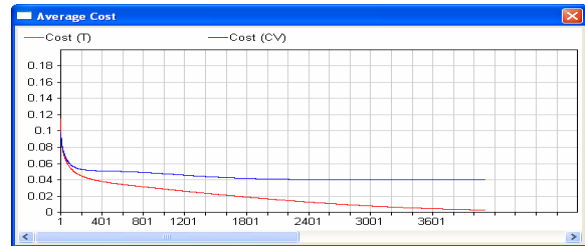


Fig. 5. The error values on the training and the cross-validation sets

TABLE II  
THE CONFUSION MATRIX FOR THE 5 TASKS CLASSIFICATION CASE

		Assigned classes				
		T1	T2	T3	T4	T5
Real classes	T1	65%	15%	5%	8.3%	6.7%
	T2	11.9%	64.2%	3.1%	8.9%	11.9%
	T3	7.6%	3.9%	78.5%	6.3%	3.7%
	T4	8.3%	8.3%	10%	70%	3.4%
	T5	7.3%	7.3%	11.8%	1.5%	72.1%

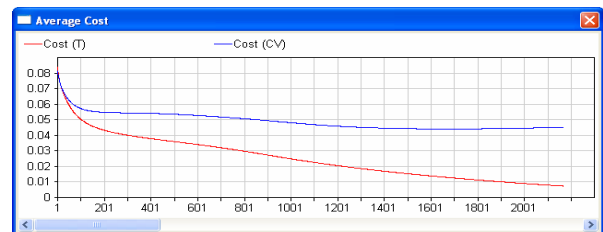


Fig. 6. The error values on the training and the cross-validation sets

The learning characteristics on training and cross-validation (CV) sets are presented in the associated figures, Fig. 5 and Fig. 6. As one can see, the error values on the both data sets (training, CV) are smoothly decaying during the learning process, one closely following the other, without oscillating. This proves that the ANN was capable to learn the feature space characteristics. The correct classification rates obtained for the case of 4 tasks classification problem were, in average, 78.275%, all of them being greater then 72%. For the case of 5 tasks classification the average correct classification rate was around 70%, each individual classification rate being greater then 64%. These are quite very good results if we take into consideration the results reported in the literature, on the

same EEG database. Thus, in [28] the average percentage of test segments correctly classified ranged from 71% for one subject (our subject) to 38% for another subject, and for the 5 tasks classification case. One can say that this is very similar with our result but actually this is not the case. The 71% correct classification performance was artificially improved within a post-processing stage when averaging across 20 consecutive segments was performed, the real value being in fact 54%. Regarding the most part of the papers dedicated to the mental tasks classification, these are focused only on pairs of mental tasks, in which case the performances take values between 70% and over 90% correct classification rates. But, these performances are decreasing with the increasing number of the analyzed mental tasks. Moreover, it was proved [27] that it is equally important to choose suitable pairs of mental tasks for each individual as compared to the feature extraction method in order to get a successful BCI design. Thus it was pointed the fact that even for the same subject, for different pairs of mental tasks one can get not very good classification results due to the subject's cognitive particularities.

#### IV. CONCLUSION

The main application for this research was the improvement of brain computer interface (BCI) systems by providing a new method for EEG feature extraction. Since we could compare our results with the results obtained on the same subject and for the same tasks and because we used the same type of classifier (MLP) as the others have done, we can conclude that the better results achieved by us are justified by one or by both of the two possible sources: 1) the new implemented EEG feature extraction technique (the EEG coherence based AAPP model) and 2) to the use of the spectral information embedded within the high gamma frequency band.

#### ACKNOWLEDGMENT

The Grant 2735/2007, theme 58, code CNCSIS 17 of the National University Research Council has supported the research for this paper.

#### REFERENCES

- [1] K. H. Kim, S. W. Bang, and S. R. Kim, "Emotion Recognition System Using Short-Term Monitoring of Physiological Signals", *Med. & Biolog. Eng. & Comput.*, vol. 42, pp. 419-427, 2004
- [2] J. M. Heasman, T. R. D. Scott, L. Kirkup, R. Y. Flynn, V. A. Vare, and C. R. Gschwind, "Control of a Hand Grasp Neuroprosthesis Using an Electroencephalogram-Triggered Switch: Demonstration of Improvements in Performance Using Wavepacket Analysis", *Med. & Biolog. Eng. & Comput.*, vol. 40, pp. 588-593, 2002
- [3] J. del R. Millán, F. Renkens, J. Mouríño, and W. Gerstner, "Noninvasive Brain-Actuated Control of a Mobile Robot by Human EEG", *IEEE Trans. on Biomed. Eng.*, vol. 51, no. 6, pp. 1026-1033, 2004
- [4] U. Hoffmann, J.M. Vesin, T. Ebrahimi, and K. Diserens, "An Efficient P300-Based Brain-Computer Interface for Disabled Subjects", *Neurosci. Met.*, 2007, [http://www.ncbi.nlm.nih.gov/sites/entrez?cmd=Retrieve&db=pubmed&dopt=AbstractPlus&list\\_uids=17445904](http://www.ncbi.nlm.nih.gov/sites/entrez?cmd=Retrieve&db=pubmed&dopt=AbstractPlus&list_uids=17445904)
- [5] E. Gysels, and P. Celka, "Phase Synchronization for the Recognition of Mental Tasks in a Brain-Computer Interface", *IEEE Trans. on Neural Sys. and Rehab. Eng.*, vol. 12, no. 4, pp. 406 - 415, 2004
- [6] M. Teplan, "Fundamentals of EEG Measurement", *Meas. Sci. Rev.*, vol. 2, Sect. 2, pp. 1-11, 2002
- [7] K. Tavakolian, A. M. Nasrabadi, and S. Rezaei, 'Selecting Better EEG channels for classification of Mental Tasks', In the Proceedings of the IEEE Int. Sym. On Circ. and Syst. ISCAS2004, pages 537-540,

- Vancouver, Canada, May 2004
- [8] K. Tavakolian, "Investigation and Comparison of Different Mental Task Classification by Linear and Nonlinear Techniques Applied to EEG Signal", Master of Science thesis, Dep. of Elect. and Comp. Eng., Univ. of Tehran, July 2003
- [9] W.Y. Hsu, C.C.Lin, M.S. Ju, Y.N. Sun, "Wavelet-Based Fractal Features with Active Segment Selection: Application to Single-Trial EEG Data", *J. of Neurosci. Met.*, vol. 163, no. 1, pp. 145-160, 2007
- [10] S. Rezaei, K. Tavakolian, A. M. Nasrabadi, and S. K. Setarehdan, "Different Classification Techniques Considering Brain Computer Interface Applications", *J. of Neur. Eng.*, vol. 3, pp. 139-144, 2006
- [11] F. Lotte, M. Congedo, A. Lécuyer, F. Lamarche, and B. Arnaldi, "A Review of Classification Algorithms for EEG-Based Brain-Computer Interfaces", *J. of Neur. Eng.*, vol. 4, no. 2, R1-R13, 2007
- [12] C. Guger, A. Schlögl, C. Neuper, D. Walterspacher, T. Strein, and G. Pfurtscheller, "Rapid Prototyping Of An EEG-Based Brain-Computer Interface (BCI)", *IEEE Trans. on Neural Sys. and Rehab. Eng.*, vol. 9, no. 1, pp. 49-58, 2001
- [13] D.P. Burke, S.P. Kelly, de P. Chazal, R.B. Reilly, and C. Finucane, "A Parametric Feature Extraction and Classification Strategy for Brain-Computer Interfacing", *IEEE Trans. on Neural Sys. and Rehab. Eng.*, vol. 13, no. 1, pp. 12-17, 2005
- [14] E. Gysels, and P. Celka, Phase synchronization for the recognition of mental tasks in a brain-computer interface, *IEEE Trans. on Neural Syst. and Rehab. Eng.*, vol. 12, no. 4, 2004, pp. 406 - 415
- [15] Q. Wei, Y. Wang, X. Gao, and S. Gao, "Amplitude and phase coupling measures for feature extraction in an EEG-based brain-computer interface", *J. of Neu. Eng.*, vol. 4, no.2, pp. 120-129, 2007
- [16] M.C. Serban, and D.M. Dobrea, "A Tremor Model Selection Based on Artificial Neural Networks Correct Classification Rate", in *Proc. of the 3rd Eur. Med. and Biol. Eng. Conf., IFMBE Proceedings*, vol. 11, pp. 3260-3265, 2005
- [17] J.R. Wolpawa, N. Birbaumer, D.J. McFarlanda, G. Pfurtschellere, and T.M. Vaughan, "Brain-Computer Interfaces For Communication And Control", *Clin. Neurophys.*, vol. 113, pp. 767-791, 2002
- [18] Hailong Liu, Jue Wang, and Chongxun Zheng, "Using Self-organizing Map for Mental Tasks Classification in Brain-Computer Interface", in *Adv. in Neural Net.*, Springer Berlin, Heidelberg, vol. 3497, pp. 327-332, 2005
- [19] K. Tavakolian, S. Rezaei, and S.K. Setarehdan, "Choosing Optimal Mental Tasks for Classification in Brain Computer Interfaces", in *Proceeding (411) Art. Intel. and App.*, 2004
- [20] C.W. Anderson web page: <http://www.cs.colostate.edu/~anderson/>, Graz dataset: <http://ida.fraunhofer.de/projects/bci/competition>
- [21] H. Liu, J. Wang, C. Zheng and P. He, "Study on the Effect of Different Frequency Bands of EEG Signals on Mental Tasks Classification", in *Proc. of the IEEE Eng. in Med. and Biol. 27th Annual Conf.*, Shanghai, China, pp. 5369-5372, 2005
- [22] R. Palaniappan, "Brain Computer Interface Design Using Band Powers Extracted During Mental Tasks", 2nd International IEEE EMBS Conf. on Neural Eng., Arlington, Virginia, pp. 321-324, 2005
- [23] E. Gysels, and P. Celka, "Phase Synchronization for the Recognition of Mental Tasks in a Brain-Computer Interface", *IEEE Trans. on Neural Syst. and Rehab. Eng.*, vol. 12, no. 4, pp. 406-415, 2004
- [24] Nai-Jen Huan et al, "Neural Network Classification of Autoregressive Features from Electroencephalogram Signals for Brain-Computer Interface Design", *J. of Neural Eng.*, vol. 1, pp. 142-150, 2004
- [25] O. Bai, M. Nakamura, A. Ikeda, and H. Shibasaki, "Nonlinear Markov Process Amplitude EEG Model for Nonlinear Coupling Interaction of Spontaneous EEG", *IEEE Trans. on Biomed. Eng.*, vol. 47, no. 9, pp. 1141-1146, 2000
- [26] H. Al-Nashash, Y. Al-Assaf, J. Paul, and N. Thakor, EEG Signal Modeling Using Adaptive Markov Process Amplitude, *IEEE Trans. on Biomed. Eng.*, vol. 51, no. 5, pp. 744-751, May 2004
- [27] R. Palaniappan, "Utilizing Gamma Band to Improve Mental Task Based Brain-Computer Interface Design", *IEEE Trans. on Neural Sys. and Rehab. Eng.*, vol. 14, no. 3, pp. 299-303, 2006
- [28] C.W. Anderson, and Z. Sijerčić, "Classification of EEG Signals from Four Subjects During Five Mental Tasks", *Proc. of the Conference on Eng. App. in Neural Net*, pp. 407-414, 1996, 1996
- [29] S. Haykin, "Neural Networks – A comprehensive Foundation", 2<sup>nd</sup> ed., Prentice-Hall Inc., New Jersey, 1999